



Lasing of a single crystal Nd³⁺ fluoride fiber

Jonas Jakutis Neto*, Tiago dos Santos Moura, Fernando Rodrigues da Silva, Sonia Licia Baldochi, Niklaus Ursus Wetter

Centro de Lasers e Aplicações, Instituto de Pesquisas Energéticas e Nucleares – Av. Professor Lineu Prestes, 2242, São Paulo – SP, Brazil

ARTICLE INFO

Article history:

Received 12 March 2010

Received in revised form 28 April 2010

Accepted 29 April 2010

Keywords:

Fiber lasers

Diode-pumped lasers

Neodymium lasers

ABSTRACT

We present laser action in a single crystal fluoride fiber obtained by the micro-pulling-down technique. The 700 μm diameter and 1 cm long Nd:LiYF₄ fiber was pumped by a beam shaped diode bar emitting at 806 nm. A peak power of 300 mW was achieved with a slope efficiency of 12%. When considering the pump power fraction absorbed by the laser mode, a slope efficiency of 37% was achieved. To the best of our knowledge, this is the first report of a Nd: LiYF₄ fiber laser.

© 2010 Elsevier B.V. All rights reserved.

1. Introduction

Single crystal fiber lasers hold the premise of combining the advantages of bulk crystals with their high emission cross sections and good thermal conductivity and fiber lasers [1,2], with their inherent capability of maintaining high pump intensities over relatively long distances, good beam quality and good thermal management. By producing thin and long fiber crystals with low doping concentration it is possible to benefit from the pump guiding and very effective heat removal properties due to a high surface to volume ratio and, at the same time, benefit from the spectroscopic and thermo-mechanical advantages of bulk crystals. Single crystal fibers can be produced with less material and the fabrication process is much faster and less costly than other methods traditionally used to grow crystals, such as the Czochralski method.

The first power scalable lasers using mini-rods of 1.5 mm [3,4] and 0.45 mm [5] diameter in an end-pumped configuration originated in the 1970s. However, the thinner the rods became, the more difficult was their preparation from bulk crystals. The alternative was single crystal fiber growth techniques. The first works used single crystal fibers doped with neodymium. Laser action was achieved mainly in Nd:YAG [6,7] and Nd:Y₂O₃ [8] fibers pumped with light-emitting diodes (LED) and with krypton lasers. Today, laser heated pedestal growth (LHPG) [9] and micro-pulling down (μPD) [10] are the most used techniques. Monocrystalline oxide fiber lasers achieve the same efficiencies as their bulk counter parts [11] due to improvements in growth techniques that provide high optical quality fibers. Recent works with oxide materials resulted in highly efficient laser action in

Nd:YAG [12] and Nd:YVO₄ [11] fibers, using the μPD and LHPG growth methods, respectively. Both techniques can be modified to permit growth of a single or double fiber cladding in order to achieve light guiding and allow integration into existing fiber technologies [13,14].

Neodymium doped LiYF₄ (Nd:YLF) has been extensively used in solid state lasers due to some favorable characteristics such as its natural birefringence, which grants polarized output, its small thermal lens that provides for good beam quality and its long upper laser level lifetime when compared to other commonly used crystal hosts such as Nd:YAG and Nd:YVO₄ [15]. Nd:YLF emits at 1047 nm when polarized along the *c*-axis (π -emission) and at 1053 nm when polarized along the other two axes (σ -emission) allowing in principle for growth of dual-wavelength polarization preserving fiber amplifiers. Its long lifetime permits a high energy storage capacity making it an attractive medium for Q-switched lasers and amplifier applications in the near-infrared region.

2. Fiber growth and analysis

A Nd:YLF fiber approximately 3 cm and with a diameter of 700 μm was grown in a μPD system specially adapted to the growth of fluoride single crystal fibers following procedures already described [16,17]. Part of the Nd:LiYF₄ fiber was pulverized for X-ray powder diffraction analysis. The measured diffractogram was compared to a standard database (ICSD 106915) [18]. The analysis showed the presence of only one single phase in the powder, corresponding to YLF single crystal structure (Fig. 1a).

A transparent portion of 1 cm length was selected for the laser experiments, cleaved and lightly polished at its end facets. The Nd³⁺ concentration as a function of the fiber length was measured by energy dispersive X-ray analysis (EDX) and is shown in Fig. 1b. A doping gradient was observed along the total fiber length, decreasing

* Corresponding author.

E-mail address: jonasjakutis@gmail.com (J.J. Neto).

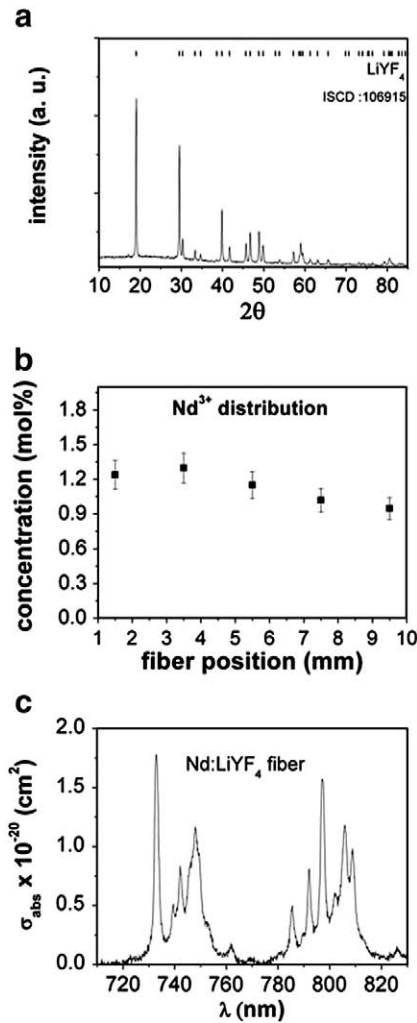


Fig. 1. Nd:YLF fiber characterization: (a) X-ray powder diffraction analysis, lines above the spectrum are the reference data, (b) neodymium concentration along the fiber (c) absorption cross section of the fiber.

from 1.2 mol% Nd^{3+} at the higher doped end facet to 0.9 mol% at the other end facet. This is an indication for a segregation coefficient in Nd:YLF of less than one [17].

The measured σ -absorption cross section of this fiber at 806 nm is $1.2 \times 10^{-20} \text{ cm}^2$, as shown in Fig. 1c, which is close to the value of bulk crystal with 1.0 mol% of neodymium ($1.7 \times 10^{-20} \text{ cm}^2$) [19]. The measured upper laserlevel (${}^4\text{F}_{3/2}$) lifetime was 390 μs for the fiber, which is smaller than the lifetime for 1 mol% of neodymium doped bulk crystal (460 μs) [17]. This fluorescence quenching is caused by cross relaxations between neodymium ions.

To show the single crystal nature over the whole fiber length and crystallographic orientation, a piece of Nd:YLF fiber was placed between two crossed polarizers at an angle of 45° with respect to the polarization axes. Due to its birefringence, this causes the fiber to become dark upon rotation around its growth axis only if the c-axis is constant throughout the sample and exactly aligned ($\pm 2^\circ$) orthogonally to the plane of the polarizers (Fig. 2a and b). Fig. 2c shows the polished endfacet of the crystalline fiber used in the laser experiments.

3. Laser characterization

The fiber was mounted on a copper heat sink (2 mm shorter than the fiber) using thermal paste for improved cooling and placed inside a plane-concave resonator with a high reflector (HR at 1047 nm and 1053 nm) of radius of curvature 25 mm and 75% transmission at the

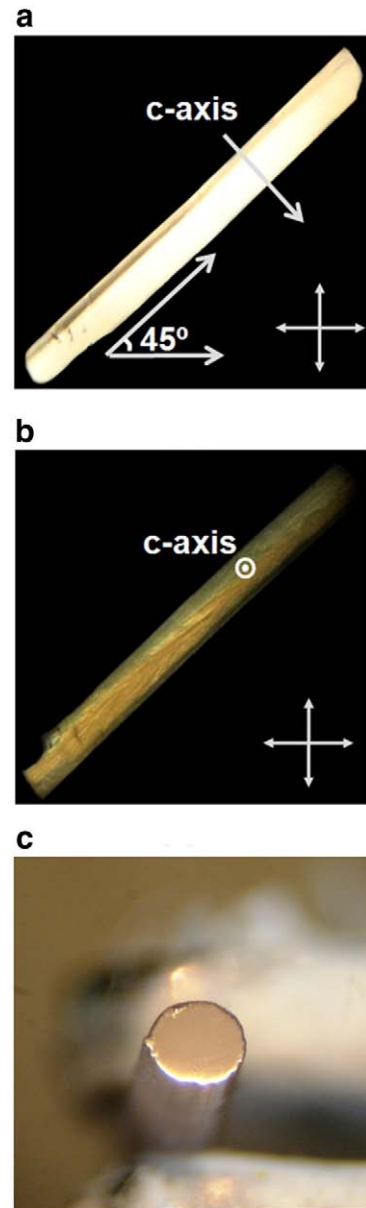


Fig. 2. Nd:YLF fiber positioned between crossed polarizers at 45° to the polarization axes (a) fiber c-axis parallel, (b) perpendicular to plane of polarizers and (c) polished crystal fiber used for laser experiments.

pump wavelength. Flat output couplers with different transmissions at the laser emission wavelength were used to characterize the laser. The calculated average TEM_{00} beam diameter inside the fiber was 132 μm , using the index of refraction for π -emission, which is 1.47 (1.45 for σ -emission). Of the several index matching fluids available at the refractive index of YLF, glycerin was chosen to optically contact the fiber to the mirrors, because of its good optical quality and low absorption at the pump and emission wavelengths. Fig. 3 shows the fiber laser setup.

The 40 W diode laser bar, used to pump the fiber, was thermally stabilized to emit at 806 nm using a temperature controller and a feedback loop. The wavelength of 806 nm was preferred as opposed to the higher absorption cross-section wavelengths of 797 nm and 792 nm because of a better thermal pump distribution. The diode emission passed through beam shaping optics that reconfigured its highly asymmetric emission into a beam with almost equal dimensions and M^2 factors in the horizontal and vertical directions [20]. The beam was focused into the fiber with a spherical lens of 50 mm focal

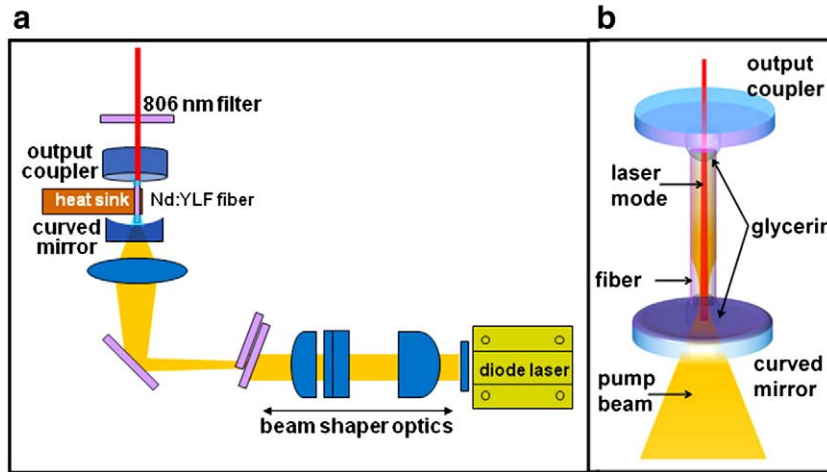


Fig. 3. (a) Fiber laser setup, (b) shows the coupling between pump beam and laser mode.

length, slightly tilted around the horizontal axis in order to compensate for astigmatism introduced by the beam shaper. The focus dimensions at the fiber facet were $250\ \mu\text{m} \times 350\ \mu\text{m}$ in the horizontal and vertical direction, respectively. The diode was operated in a quasi-continuous (qcw) mode with 2 ms pulse duration and 6.5% duty cycle to avoid fiber fracture. Continuous operation was not investigated given the small thermal fracture limit of Nd:YLF (which is five times smaller than in Nd:YAG [21]) and the lack of refrigeration in our setup. A pump power fraction of 98% was absorbed inside the fiber as measured with a power meter (Coherent, model PS19). This fraction includes scattering losses caused by fiber defects.

The fiber's transmission loss and small signal gain were characterized by changing the cavity mirrors to flat BK7 substrates and using a TEM₀₀, 1053 nm laser probe beam from a homemade Nd:YLF laser. The probe beam was focused through a 30 cm lens into the fiber end that is opposite to the pump end ($47\ \mu\text{m}$ beam radius at focus inside fiber). A loss coefficient of $\alpha = 0.019\ \text{cm}^{-1}$ corresponding to a single pass loss of $1.90 \pm 0.3\%$ was measured. The small signal gain was obtained by pumping the fiber with the pump system described in Fig. 3. At a laser probe beam power of 111 mW, corresponding to an intensity of $1.60\ \text{kW}/\text{cm}^2$ inside the fiber, and a pump power of 8.5 W at 806 nm, a gain coefficient of $0.104 \pm 0.018\ \text{cm}^{-1}$ (gain minus loss) was measured. A small signal gain coefficient of $0.19\ \text{cm}^{-1}$ (non-saturated single pass gain of 21%) was calculated, using a saturation intensity of $3.14\ \text{kW}/\text{cm}^2$ for Nd:YLF at 1053 nm.

The pump guiding efficiency of the fiber was qualitatively evaluated, too. First, a large area power detector was positioned immediately behind the fiber end that is opposite to the pump end and the transmitted power was measured. Then, a pinhole with the same diameter as the fiber was positioned in contact to the fiber end closest to the power detector. This pinhole blocked all radiation leaving the fiber through the cylindrical surface. A fraction of 68% of the remaining pump light escaped through the fiber end facet. This shows clearly that pump guiding is present and strong, considering the average divergence of 24° of the pump beam, which completely fills the fiber after only 2 mm of propagation.

The fiber was aligned with its *c*-axis parallel to the diode laser's TM-polarized output beam, although there is no significant difference in absorption coefficients for π - or σ -polarization at the pump wavelength of 806 nm. The laser output power was detected (Coherent, model OP-2 VIS) using a filter to block the 806 nm pump radiation that transmitted 65% at 1053 nm. Beam quality was accessed by a CCD camera (Newport, model LBP-4) and also using the knife edge method to measure the M^2 value [22].

Different flat output coupler transmissions were tested. The other mirror had radius of curvature (ROC) of 2.5 cm and cavity length was

1.1 cm. Fig. 4a shows the output power as a function of the mirror reflectivity for three different transmissions. Employing a Findlay–Clay analysis [23], round-trip losses of $2.00 \pm 0.05\%$ (1.0% single pass)

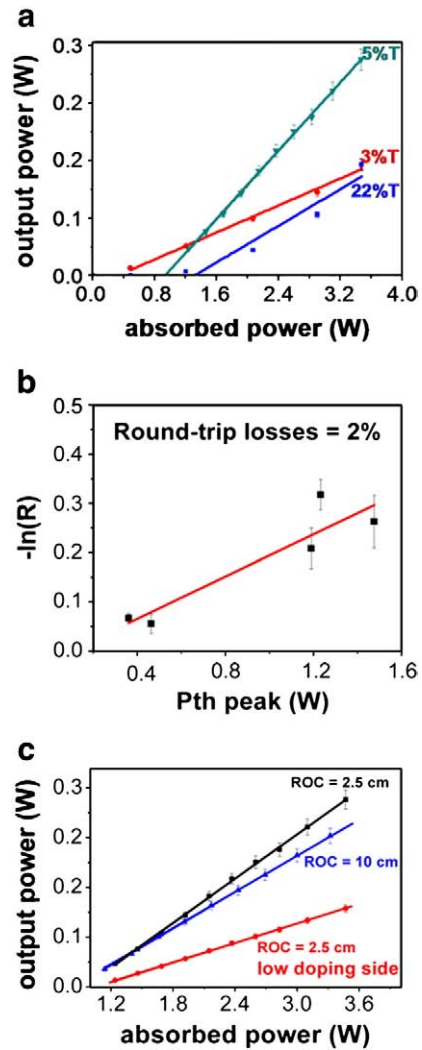


Fig. 4. Laser characterization. (a) Output power versus input power for different transmissions of the flat output coupler (the other mirror has ROC of 2.5 cm). (b) Findlay–Clay analysis and (c) Output power as a function of radius of curvature of the mirror at 5% output coupler transmission.

were calculated for this cavity, as shown in Fig. 4b. Similarly, a CAIRD-analysis resulted in a round-trip loss of $4.1 \pm 0.4\%$ which is closer to the previously obtained single pass loss of 1.9% [24]. Fitting the output power data as a function of output coupling with a low gain approximation [15], a single pass small signal gain coefficient of 0.54 cm^{-1} was obtained using above calculated saturation intensity and a round-trip loss of 4% .

We also tested different radii of curvature for the input coupling mirror, as shown in Fig. 4c. The highest slope efficiency of 12% was obtained for a ROC of 2.5 cm (calculated mode radius of $68 \mu\text{m}$ inside fiber) when pumping the fiber through the higher doped end facet. When pumping the other facet, the efficiency dropped to 5.2% . Using a ROC of 10 cm (laser mode radius $87 \mu\text{m}$) and pumping the higher doped end facet, the efficiency dropped to 9.7% . All these measurements were done with a 5% transmission, flat output coupler. The absorbed pump power is the total power absorbed by the fiber.

Laser oscillation was observed on both (π and σ) transitions as shown in Fig. 5a [25]. Small mirror tilts resulted in stable operation for only one wavelength (π or σ) or both wavelengths simultaneously. The power stability is directly related to the wavelength stability. When the resonator is aligned for only one polarization (π or σ polarization), the laser power becomes stable. The highest output power of 301 mW (19.5 mW of average output power) was achieved when the cavity was optimized for 1047 nm lasing without simultaneous σ -lasing using an

output coupler with 5.0% transmission and a ROC of 2.5 cm (Fig. 4c). The measured output beam quality at this output power was $M^2 = 3.1 \times 2.4$ in the horizontal and vertical directions, respectively.

TEM₀₀ mode oscillation was also achieved in this fiber at a slightly lower output power of 193.2 mW and at an emission wavelength of 1053 nm (Fig. 5c). The optical-to-optical efficiency in fundamental mode was 5.3% and the corresponding slope efficiency was 6.4% . The measured M^2 factor was 1.26×1.02 in the horizontal and vertical directions, respectively, as shown in Fig. 5b.

4. Discussion

The measured single pass loss of 1.9% in the Nd:YLF fiber is higher than in bulk material, but still low enough to permit efficient lasing. On the other hand, the efficiency obtained of 12% (see curves in Fig. 4a and c, with 5% transmission and ROC 2.5 cm , respectively) is lower than that obtained in bulk crystals (53%) [26,27]. This is mainly due to the poor overlap between laser beam and pump beam. Indeed, the overlap integrated absorption efficiency, which gives the pump power fraction absorbed by the oscillating laser mode, is only 29.8% [28]. Therefore, the slope efficiency as a function of the pump power absorbed by the laser mode is much higher, that is 37% which is much closer to the optimum of 53% obtained in bulk crystals. The small intracavity TEM₀₀ mode, given by the 25 mm ROC of the pump mirror, was chosen in order to optimize gain and to permit choosing the best region inside the fiber having in mind the fiber's imperfections close to the border (see Fig. 1). The necessity of using a small mode inside the fiber in order to escape imperfections is confirmed by the fact that the 10 cm ROC mirror that causes a larger beam waist ($78 \mu\text{m}$ as compared to $68 \mu\text{m}$ using the 2.5 cm ROC mirror) and, therefore, in principle has better overlap with the pump beam, does present a smaller gain (Fig. 4c). Pumping the highly doped side causes higher gain (Fig. 4c), as expected, because, in our configuration, good overlap between both beams is only obtained at the beginning of the fiber.

Longer fibers have been pulled and future works intend to use the full concept of fiber laser with long lengths and low doping concentration in order to obtain efficient and power scalable Nd:YLF fiber lasers. Additionally we are investigating the possibility to grow the fiber with cladding using two concentric capillaries during the growth process [29]. Growing the fiber with cladding should also permit higher duty cycles and cw operation because the fiber could be effectively refrigerated with cooling liquid or by conductive cooling using i.e. indium foil.

5. Conclusions

Fluoride fibers are difficult to grow with high quality which is demonstrated by the fact there is only one other demonstration fluoride crystalline fiber lasers [30]. Nevertheless, the distinct advantages of bulk Nd:YLF lasers, cited in the introduction, make it worthwhile to pursue the task of achieving high quality Nd:YLF crystalline fibers. Here, we demonstrate for the first time lasing in a single crystal Nd:YLF fiber grown by the micro-pulling-down technique obtaining a slope efficiency of 12% .

Acknowledgements

We thank foundation FAPESP for grants 05/53241-9 and 06/563713 and the national science council CNPq.

References

- [1] J. Limpert, F. Roser, S. Klingebiel, T. Schreiber, C. Wirth, T. Peschel, R. Eberhardt, A. Tunnermann, IEEE J. Sel. Top. Quantum Electron. 13 (2007) 537.
- [2] A.W. Al-Alimi, M.H. Al-Mansoori, A.F. Abas, M.A. Mahdi, M. Ajiya, Laser Phys. Lett. 6 (2009) 727.
- [3] F.W. Ostermayer Jr., R.B. Allen, E.G. Dierschke, Appl. Phys. Lett. 19 (1971) 289.

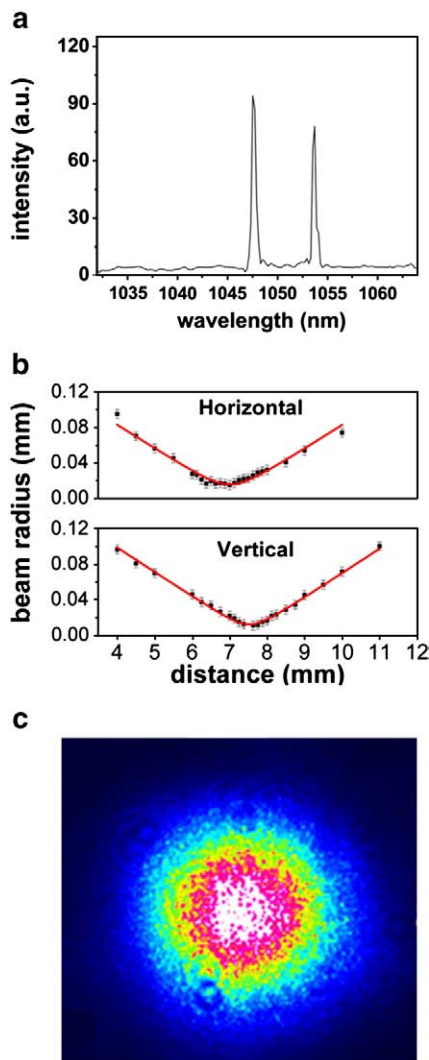


Fig. 5. (a) Simultaneous oscillation of π and σ polarization (b) M^2 measurements of this beam and (c) CCD record of TEM₀₀ laser beam profile.

- [4] L.J. Rosenkrantz, *J. Appl. Phys.* 43 (1972) 4603.
- [5] R.B. Chesler, D.A. Draeger, *Appl. Phys. Lett.* 23 (1973) 235.
- [6] C.A. Burrus, J. Stone, *Appl. Phys. Lett.* 26 (1975) 318.
- [7] J. Stone, C.A. Burrus, A.G. Dentai, B.I. Miller, *Appl. Phys. Lett.* 29 (1976) 37.
- [8] J. Stone, C.A. Burrus, *J. Appl. Phys.* 49 (1978) 2281.
- [9] R.S. Feigelson, E. Caldis, *Crystal Growth of Electronic Materials*, Elsevier Science, Amsterdam, 1985.
- [10] T. Fukuda, V.I. Chani, *Shaped Crystals: Growth by Micro-Pulling-Down Technique*, Springer, Berlin, 2007.
- [11] A.S.S. de Camargo, L.A.O. Nunes, D.R. Ardila, J.P. Andreetta, *Opt. Lett.* 29 (2004) 59.
- [12] J. Didierjean, M. Castaing, F. Balembois, P. Georges, D. Perrodin, J. Fourmigué, K. Lebbou, A. Brenier, O. Tillement, *Opt. Lett.* 31 (2006) 3468.
- [13] B.M. Epelbaum, K. Inaba, S. Uda, K. Shimamura, M. Imaeda, V.V. Kochurikhin, T. Fukuda, *J. Cryst. Growth* 179 (1997) 559.
- [14] C.C. Lai, H.J. Tsai, K.Y. Huang, K.Y. Hsu, Z.W. Lin, K.D. Ji, W.J. Zhuo, S.L. Huang, *Opt. Lett.* 33 (2008) 2919.
- [15] W. Koehner, *Solid-State Laser Engineering*, Springer, Berlin, 1996, p. 89.
- [16] A.M.E. Santo, I.M. Ranieri, G.C.S. Brito, B.M. Epelbaum, S.P. Morato, N.D. Vieira Jr., S.L. Baldochi, *J. Cryst. Growth* 275 (2005) 528.
- [17] A.M.E. Santo, A.F.H. Librantz, L. Gomes, P.S. Pizani, I.M. Ranieri, N.D. Vieira Jr., S.L. Baldochi, *J. Cryst. Growth* 292 (2006) 149.
- [18] H. de Leebeeck, K. Binnemans, C. Goerler Walrand, *J. Alloy. Comp.* 291 (1999) 300.
- [19] Z. Ma, J. Gao, D. Li, J. Li, N. Wu, K. Du, *Opt. Commun.* 281 (2008) 3522.
- [20] N.U. Wetter, *Opt. Laser Tech.* 33 (2001) 181.
- [21] W.A. Clarkson, P.J. Hardman, D.C. Hanna, *Opt. Lett.* 23 (1998) 1363.
- [22] E. Siegman, M.W. Sasnett, T.F. Johnston, *IEEE J. Quant. Electron.* 27 (1991) 1098.
- [23] D. Findlay, R.A. Clay, *Phys. Lett.* 20 (1966) 277.
- [24] J.A. Caird, S.A. Payne, P.R. Staver, A.J. Ramponi, L.L. Chase, L.F. Krupke, *IEEE J. Quant. Electron.* 24 (1988) 1077.
- [25] B. Frei, J.E. Balmer, *Appl. Opt.* 33 (1994) 6942.
- [26] J. Zehetner, *Opt. Commun.* 117 (1995) 273.
- [27] N.U. Wetter, E.C. Sousa, I.M. Ranieri, S.L. Baldochi, *Opt. Lett.* 34 (2009) 292.
- [28] K. Kubodera, K. Otsuka, *J. Appl. Phys.* 50 (1979) 653.
- [29] C.C. Lai, H.J. Tsai, K.Y. Huang, K.Y. Hsu, Z.W. Lin, K.D. Ji, W.J. Zhuo, S.L. Huang, *Opt. Lett.* 33 (2008) 2919.
- [30] M.H. Pham, M.M. Cadatal, T. Tatsumi, A. Saiki, Y. Furukawa, T. Nakazato, E. Estacio, N. Sarukura, T. Suyama, K. Fukuda, K.J. Kim, A. Yoshikawa, F. Saito, *Jpn. J. Appl. Phys.* 47 (2008) 5605.